Int. J. Solids Structures Vol. 27, No. 13, pp. 1623–1637, 1991
Printed in Great Britain.

0020-7683/91 $3.00 + .00

ON MULTIPLE DELAMINATION BUCKLING AND GROWTH IN COMPOSITE PLATES

PER-LENNART LARSSON
Department of Solid Mechanics, Royal Institute of Technology, S-100 44 Stockholm, Sweden

(*Received* 27 *September* 1989; *in revised form* 29 *June* 1990)

Abstract—Composite plates containing a multiple number of delaminations are analyzed with respect to combined buckling and crack growth. The von Karman plate theory is employed to determine axisymmetric bifurcation and post-buckling behavior, in particular with respect to contact between delaminated layers. For various combinations of geometry and material parameters, energy release rates at incipient crack growth are determined and stability characteristics predicted. The results show that contact between buckled layers may significantly influence post-buckling features and promote delamination growth.

1. INTRODUCTION

Composite panels composed of laminates are currently used as structural members in many applications, mainly to ensure properties of some optimal design. In order to secure a satisfactory service life, however, the structural integrity of laminates has to be duly considered. A notorious issue in this context has been concerned with the presence of interlaminar cracks or delaminations. Thus, the origin of such damage may lead to severe degradation of stiffness and strength of load-carrying members such as in aircraft structures. Some of these issues have recently been discussed in a survey by Storåkers (1989), which for one thing emphasized the need for analyzing problems concerning multiple delaminations. The particular type of damage involved seems to be especially frequent at low velocity impact.

When analyzing laminates under external loading and containing multiple delaminations, circumstances might become very complex, as illustrated in Fig. 1a. Thus, the features of buckling and crack propagation are likely to be much involved, especially when contact between laminates occurs and possibly also because of fiber failure and kinking of cracks. However, for less complicated crack patterns, as illustrated in Fig. 1b, Chai *et al.* (1981) have produced results which are simplified though still of practical importance.

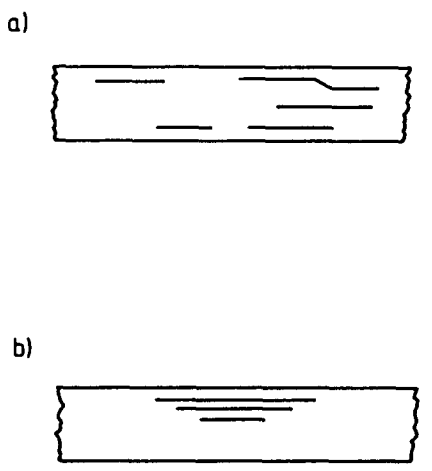

Fig. 1. Delamination damage after impact.

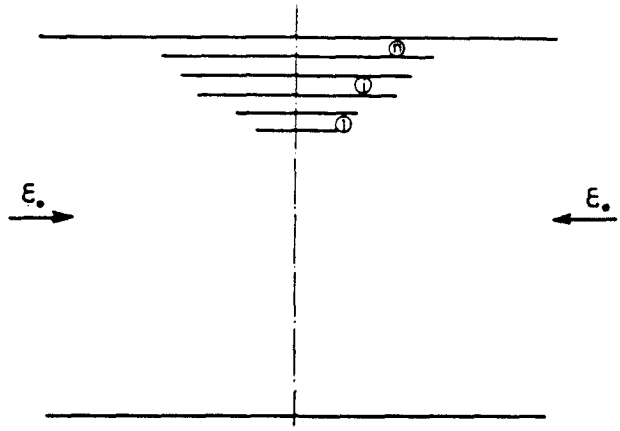

Fig. 2. Composite plate with n delaminations.

In general, problems of the type outlined have so far received little attention in the literature. Bolotin *et al.* (1981) analyzed the case of column buckling with several though non-interacting equidistant delaminations of equal length. The results were restricted to the eigenvalue problem and proved that the lowest buckling loads correspond to antisymmetric modes. Chai *et al.* (1981) analyzed the problem when one delaminated ply was thick enough to resist significant bending and considered a simplified treatment of a multiply-delaminated beam–column structure by retaining a single delamination growth. Wang *et al.* (1985a,b) also studied buckling of multiple delaminations although the analysis was restricted to symmetry and to the eigenvalue problem only, without consideration of contact.

In Fig. 2, a damaged area with multiple delaminations due to impact is depicted, according to experimental results shown in principle by Chai and Babcock (1985). The present contribution aims at solving the corresponding problem due to buckling and crack growth. Geometry and loading are assumed axisymmetric and non-frictional contact between delaminated layers is taken into account. The analysis is restricted to delaminations of consecutive magnitudes, as depicted in Fig. 2; such features frequently prevail due to impact. As regards material behavior individual delaminated layers are assumed to be linear elastic and isotropic. This, however, does not exclude anisotropic material behavior of individual laminae. It is furthermore presumed that the damaged part of the panel is thin enough so that the "thin-film" approximation (Chai *et al.*, 1981), is applicable in the analysis, i.e. bending deformation is neglected in undamaged laminated segments. It has been shown earlier by Larsson (1990) that in the case of a single delamination, very accurate results for the thin-film approximation were found for delaminated thicknesses that were less than 25% of the total panel thickness essentially, though for clamped conditions as in this presentation. It is believed then that similar circumstances will prevail as regards the present geometric details.

2. BASIC EQUATIONS FOR DELAMINATED LAYERS

The class of problems concerned involves multiple layers of circular shape. It is advisable then to first establish the potential energy for a circular plate of radius a and thickness t. Thus, for an axisymmetric and Hookean situation

$$U = \int_0^a \left[\frac{Et}{(1-\nu^2)} \left\{ \left[\frac{du}{dr} + \frac{1}{2}\left(\frac{dw}{dr}\right)^2 \right]^2 + 2\nu \left[\frac{du}{dr} + \frac{1}{2}\left(\frac{dw}{dr}\right)^2 \right] \frac{u}{r} + \left(\frac{u}{r}\right)^2 + \frac{t^2}{12}\left[\left(\frac{d^2w}{dr^2}\right)^2 + \frac{2\nu}{r}\frac{dw}{dr}\cdot\frac{d^2w}{dr^2} + \left(\frac{1}{r}\frac{dw}{dr}\right)^2 \right] \right\} - 2qw \right] \cdot \pi r \, dr \quad (1)$$

in the von Karman approximation. In (1), $q(r)$ is the transverse distributed loading and u

and w are the radial and transverse displacements, presently being prescribed at the boundary, $r = a$.

The governing equations are then generated by varying the potential in (1) and as the present situation is multiple, each variation for a delaminated layer as shown in Fig. 2 has to be considered.

At an individual layer of index j, the kinematic constraints to be satisfied at $r = a_j$ read

$$\left.\begin{aligned} u_j &= -a_j\varepsilon_0 \\ w_j &= 0 \\ \frac{\mathrm{d}w_j}{\mathrm{d}r} &= 0 \end{aligned}\right\} \tag{2}$$

as, according to the thin-film approximation, straining is homogeneous outside delaminated layers.

If contact occurs between two layers, j and $j+1$ say, then in conformity with distributed transverse displacements and loading q_{jj} between layers j and $j+1$,

$$(w_{j+1}(r) - w_j(r))q_{jj}(r) = 0 \tag{3}$$

with the restrictions

$$w_{j+1}(r) - w_j(r) \geqslant 0, \quad q_{jj}(r) \geqslant 0. \tag{4}$$

If contact is also present between the supplementary layers j and $j-1$, then the resulting pressure on the jth layer may be subsequently expressed at a point r as

$$q_j(r) = q_{j\,j-1}(r) - q_{jj}(r) \tag{5}$$

in the introduced notation.

Having accounted for the local behaviour and interaction of laminates, it now proves useful to introduce dimensionless local variables according to

$$\left.\begin{aligned} \bar{r}_j &= r/a_j \\ \bar{u}_j &= u_j a_j/t_j^2 \\ \bar{w}_j &= w_j/t_j \\ \bar{q}_j &= q_j a_j^4/(E_j t_j^4). \end{aligned}\right\} \tag{6}$$

By introducing (6) into (1), the variational equation to be solved for each individual layer reads

$$\int_0^1 \{(\bar{u}_j' + \bar{w}_j'^2/2)(\delta\bar{u}_j' + \bar{w}_j'\delta\bar{w}_j') + \nu_j[(\bar{u}_j' + \bar{w}_j'^2/2)\delta\bar{u}_j + \bar{u}_j(\delta\bar{u}_j' + \bar{w}_j'\delta\bar{w}_j')]/\bar{r}_j + (\bar{u}_j/\bar{r}_j)(\delta\bar{u}_j/\bar{r}_j)$$
$$+ [(\bar{w}_j'' + \nu_j\bar{w}_j'/\bar{r}_j)\delta\bar{w}_j'' + (\nu_j\bar{w}_j''/\bar{r}_j + \bar{w}_j'/\bar{r}_j^2)\delta w_j']/12 - (1-\nu_j^2)\bar{q}_j\delta\bar{w}_j\}\bar{r}_j\,\mathrm{d}\bar{r}_j = 0, \tag{7}$$

where a prime now and in the following represents differentiation with respect to $\bar{r}_j$.

3. SOLUTION PROCEDURE FOR BUCKLING

In order to solve the buckling and post-buckling problem as given implicitly by eqn (3), an iterative procedure based on the so-called conjugate gradient method is employed while in each iteration step a finite element method is used to determine the displacement fields $w_j(r)$.

The solution procedure is commenced by making an initial search for the contact pressure between overlapping adjacent layers. Increments for the pressure are then subsequently added until eqn (3) is satisfied everywhere in the structure.

By denoting the displacement and contact pressure of node i, layer j by $w_j(i)$ and $q_{jj}(i)$, respectively, the pressure increments at the iteration k are given by

$$q_{jj}^{k+1}(i) - q_{jj}^{k}(i) = d_j^k(i) \tag{8}$$

where

$$d_j^k(i) = -g_j^k(i) + \beta^k d_j^{k-1}(i) \tag{9}$$

and

$$\left.\begin{aligned} g_j^k(i) &= (w_{j+1}^k(i) - w_j^k(i)) \cdot q_{jj}^k(i)/t_1 \\ \beta^k &= g_j^k(i)(g_j^k(i) - g_j^{k-1}(i))/(g_j^{k-1}(i) \cdot g_j^{k-1}(i)). \end{aligned}\right\} \tag{10}$$

The resulting pressure on layer j at node i is then given by

$$q_j^{k+1}(i) = q_{jj}^{k+1}(i) - q_{jj}^{k+1}(i), \text{ as according to eqn (5).}$$

In the iteration procedure, a converging solution was considered sufficiently accurate when

$$\min((w_{j+1}(i) - w_j(i))/\max(w_{j+1})) > -\varepsilon, \tag{11}$$

where ε in no case dealt with was larger than 10^{-3}.

In order to initiate the procedure, contact between the substrate and the lowest layer was not considered. The solutions for the post-buckling displacements showed, however, that in no case analyzed was this kind of contact present. Furthermore, although no rigorous investigation was carried out as to whether potential energy minima were actually achieved, perturbations of contact pressures were performed with the intention to reasonably secure the reliability of the solution method. This issue was important in particular at crack tips since the left-hand side of (11) then becomes ambiguous by definition.

This iteration method just outlined, known as the conjugate gradient method, may be characterized as a Newton method with the Jacobian taken to be the identity matrix and a correction term $\beta^k d_j^{k-1}(i)$ added in order to improve the rate of convergence. A more detailed description of the method has been given by Strang (1986).

It remains then to consider the displacement fields $\bar{w}_j(i)$ at buckling. As the thin-film approximation is adopted, the delaminated layers will buckle initially as for a clamped circular plate. The critical edge displacement at the outer boundary then becomes in a standard manner

$$u_j^{cr}(a_j) = -1.2235 t_j^2/((1+\nu_j)a_j) \tag{12}$$

for each individual layer. The continued post-buckling displacements are then determined by solving eqn (7) via the finite element method.

In all major details, the same finite element procedure was adopted as the one used by Storåkers and Andersson (1988). Consequently the basic element trial functions, N_k, used in element i, $\bar{r}(i) \leqslant \bar{r} \leqslant \bar{r}(i+1)$, were explicitly

$$\left.\begin{aligned} N_1 &= (\xi-1)^2(\xi+2)/4, \quad N_2 = -(\xi+1)^2(\xi-2)/4, \\ N_3 &= (\xi-1)^2(\xi+1)h/8, \quad N_4 = (\xi+1)^2(\xi-1)h/8, \end{aligned}\right\} \tag{13}$$

where

$$\xi = (2\bar{r} - \bar{r}(i) - \bar{r}(i+1))/(\bar{r}(i+1) - \bar{r}(i))$$

and

$$h = \bar{r}(i+1) - \bar{r}(i).$$

For the numerical procedure it is suitable to write eqn (7) in incremental form. Replacing $\bar{u}_j$, $\bar{w}_j$ by $\bar{u}_j + \Delta u_j$, $\bar{w}_j + \Delta\bar{w}_j$ where $\Delta\bar{u}_j$ and $\Delta\bar{w}_j$ are increments sought for, yields to first order

$$\begin{pmatrix} K_{11} & K_{12} \\ K_{12}^{\mathrm{T}} & K_{22} \end{pmatrix}_j \begin{pmatrix} \Delta\bar{u}_j \\ \Delta\bar{w}_j \end{pmatrix} = \begin{pmatrix} R_1 \\ R_2 \end{pmatrix}_j \tag{14}$$

where the explicit expressions for $(K_{\alpha\beta})_j$ and $(R_\alpha)_j$ are given in Appendix A.

Expressed in this manner, the satisfaction of equilibrium corresponds in a weak sense to the vanishing of the right-hand side of eqn (14). The solution then proceeds in a standard manner through iteration of (14), where the increments $\Delta\bar{u}$ and $\Delta\bar{w}$ are added to the displacement fields $\bar{u}$ and $\bar{w}$ until the relative magnitudes of corrections in displacements and energies are less than predetermined values.

As regards the main features in the element procedure proposed by Storåkers and Andersson (1988) there exists, however, one additional issue as regards multiple laminates. Due to the presence of contact between individual layers, the $\bar{r}$-dependence of the resulting pressure $\bar{q}_i$ had to be duly considered and implemented into the numerical procedure. This was accomplished by allowing $\bar{q}_i$ to vary linearly over each element. Explicitly, the pressure $\bar{q}_i$ applied to element i, $\bar{r}_j(i) \leqslant \bar{r}_j \leqslant \bar{r}_j(i+1)$, reads

$$\bar{q}_i(\bar{r}_j) = \{\bar{q}_i(\bar{r}_j(i))\bar{r}_j(i+1) - \bar{q}_i(\bar{r}_j(i+1))\bar{r}_j(i) + (\bar{q}_i(\bar{r}_j(i+1)) - \bar{q}_i(\bar{r}_j(i)))\bar{r}_j\}/r(\bar{r}_j(i+1) - \bar{r}_j(i)) \tag{15}$$

where the node pressures $\bar{q}_j(\bar{r}_j(i))$ and $\bar{q}_j(\bar{r}_j(i+1))$ were determined by the iterative procedure just outlined.

4. THE ENERGY RELEASE RATE AT DELAMINATION GROWTH

In order to predict delamination growth, the most common criterion adopted is associated with the energy release rate as in the spirit of Griffith's classical work. When crack growth is self-similar, it is then a straightforward matter to determine the rate of change of potential energy of the system. In a general situation, however, the resistance to crack propagation may be mode-dependent and the inhomogeneity of crack parameters might become quite intricate.

Presently the issue of mode partitioning, eventually as in modes I and II for axisymmetry, will not be considered but instead local values of the energy release rate will be discussed in the spirit of Storåkers and Andersson (1988), starting from the von Karman plate theory and first principles. Thus, as found by these writers, the energy released at crack advance $\delta a(x_\alpha)$ with a crack contour Γ_c having the local normal n_α, may be expressed as

$$-\delta U = \int \| P_{\alpha\beta} \| n_\alpha n_\beta \, \delta a \, \mathrm{d}\Gamma_c \tag{16}$$

where $P_{\alpha\beta}$ may be interpreted as a plate analogue of Eshelby's energy momentum tensor and $\| \quad \|$ denotes its jump determined from the individual plate members intersecting at the crack front.

Explicitly, $P_{\alpha\beta}$ reads (Storåkers and Andersson, 1988)

$$P_{\alpha\beta} = W\delta_{\alpha\beta} - N_{\alpha\gamma}u_{\gamma,\beta} + M_{\alpha\gamma}u_{3,\gamma\beta} - Q_{\alpha}u_{3,\beta}, \tag{17}$$

where W denotes the plate strain energy density and, leaving out details, the remaining variables are conjugate quantities in a customary sense.

Once the combined post-buckling and contact problem outlined earlier has been solved, no fundamental difficulties remain by combining (16) and (17) to compute energy release rates locally at crack fronts. In the present case, the problem is technically advantageous as axisymmetry prevails. Furthermore, superposition of a homogeneous strain field ε_0 will simplify matters further as it does not affect the energy release rate but produces a stress free state in regions away from delaminated parts. This issue has been discussed in some detail by Yin (1985) and Suo and Hutchinson (1988).

5. RESULTS AND DISCUSSION

The problem of multiple delaminations subjected to buckling involves many aspects since the parameters comprised are not only due to outer loading and material constants but also crack length and thickness ratio between delaminated layers including the particular issue of contact pressure. The aim of the present investigation is, therefore, to obtain a quantitative description of the multiple delamination problem providing insight into engineering applications and especially how the presence of contact affects energy release rates and subsequent crack growth behavior. The illustrations analyzed are therefore chosen in such a way that contact occurs as otherwise the multiple delamination problem may be reduced to analyzing a number of single delaminations separately as dealt with by earlier writers.

The outer loading is introduced into the individual laminates through the parameters

$$\lambda_j = \sqrt{12(1-\nu_j^2)}|\bar{u}_j(1)|, \tag{18}$$

which corresponds to non-dimensional in-plane displacements at the crack fronts. Since λ_j in (18) is equivalent to the parameter $\bar{a}$ introduced by Yin (1985) in the analysis of single delamination problems, this facilitates a direct comparison between the present results and earlier non-contact problems.

When presenting explicit results it proves useful to introduce a dimensionless measure for the energy release rate at the crack fronts according to

$$\bar{G}_j = G_j/(E_1 t_1 \varepsilon_0^2) \tag{19}$$

in obvious notation.

With a multiple number of delaminations present in a plate structure, contact can enter the problem in a number of ways. Thus, Fig. 3a describes a straightforward contact problem to be analyzed in the following. For simplicity, initially only two delaminations are assumed to be present but the layers can, however, be made of different materials and thicknesses. In the first event considered, Figs 3a and 3b, the buckling load for the upper layer, layer 2, is smaller than that for the lower one, layer 1. As a consequence, initially no contact arises, Fig. 3a, and the interesting feature corresponds to the later event when also the lower layer starts to buckle, Fig. 3b. However, this situation does not necessarily mean that contact initially enters the problem but if transverse displacements of the lower layer are high enough, either directly or after crack growth, a contact problem will result as shown in Fig. 3b. It is clear though that if contact does not occur the problem may be dealt with as single delamination problems although both layers have deflected transversally.

In Figs 3c and 3d, the problem is posed somewhat differently since in this case the lower layer buckles first. Depending on the magnitude of the bending stiffness of the upper layer, essentially two features may occur; either the lower layer forces the upper layer to deflect substantially, Fig. 3c, or layer 2 is so stiff that there is virtually no deflection until

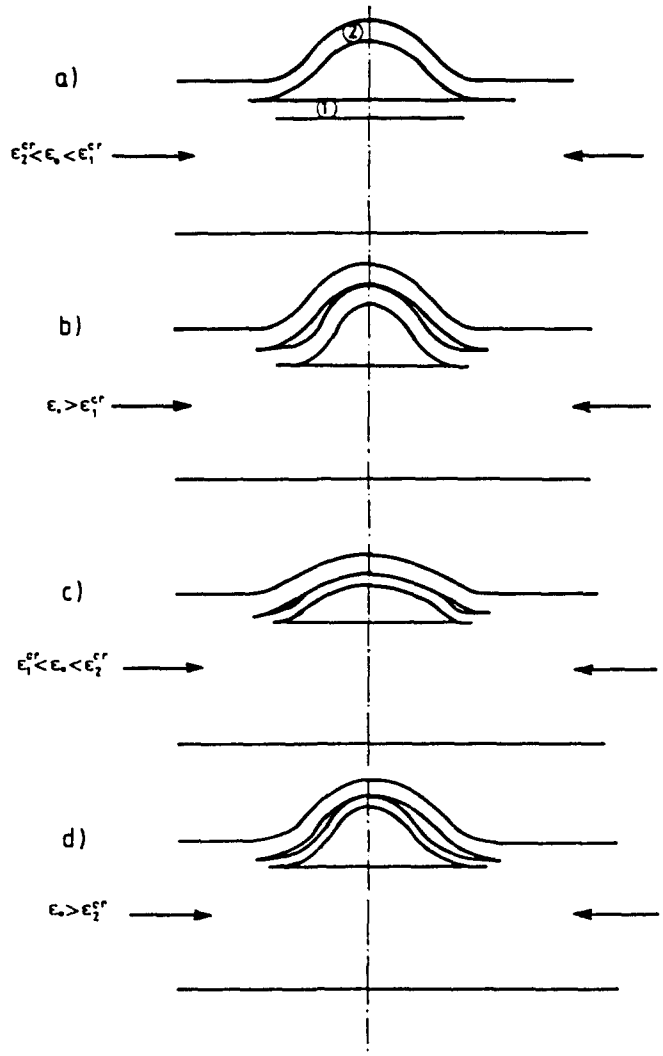

Fig. 3. Buckled delamination geometries to be analyzed.

the outer loading reaches the buckling load also for the upper layer. In any case, contact does enter the problem directly if the lower layer buckles first. At combined buckling, all the cases analyzed showed that the contact area was somewhat decreasing under external load, Fig. 3d, although contact was still maintained.

To conclude then, as regards the fundamental difference between the cases just outlined, the issue concerns the behavior of the layers, i.e. whether buckling occurs for both layers or not as in Figs 3a and 3c, respectively. As soon as both layers have buckled, the two problems as in Figs 3b and 3d are principally the same when contact is present.

The main attention is now focused on some relevant and explicit results. It seems natural then to first consider a case for which the outer loading is increased monotonically so that buckling of one layer occurs initially. Subsequently, buckling of both layers and ensuing transverse displacements in the post-buckling range enter with possibly the whole process of contact being present throughout.

In Fig. 4, the transverse displacement at the center of the layers is depicted as a function of the outer loading represented by the parameter λ_2 defined in (18). In this case two equally long cracks are considered, and the two layers are made of the same isotropic material, although the upper layer is slightly thicker than the lower one, viz. $t_2 = 1.1t_1$. This implies that the lower plate buckles first and forces the upper one to deflect before buckling, corresponding to a situation as described in Figs 3c and 3d. Nominally the upper plate

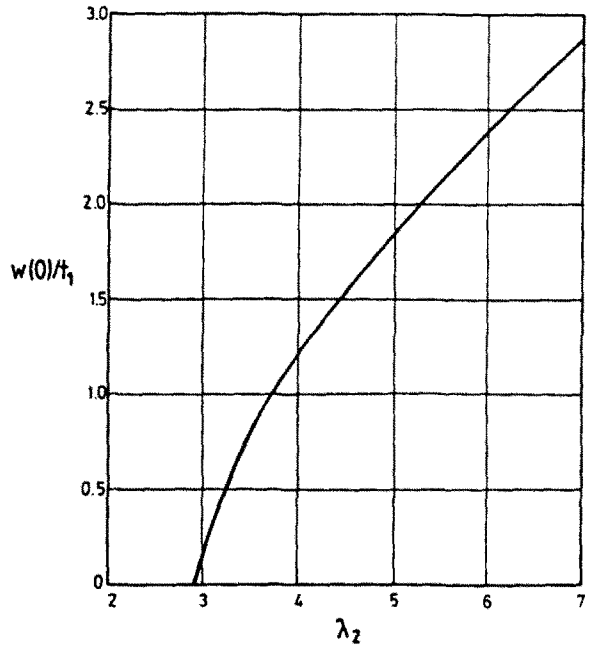

Fig. 4. Transverse displacements, $w(0)/t_1$, as a function of non-dimensional edge displacement, λ_2, for a plate with two delaminations, $E_1 = E_2$, $\nu_1 = \nu_2 = 0.3$, $a_1 = a_2$, $t_2 = 1.1t_1$.

buckles when λ_2 approximately takes on the value 3.2 and it may be observed in Fig. 4 that the ensuing load–deflection curve constitutes rather smooth behavior.

In Fig. 5 energy release rates are shown and also a comparison between the values for the upper layer from the present analysis and that by Yin (1985) for a single delamination is made. As may be seen, the energy release rate is higher for the upper layer and the difference compared to the case of a single delamination is around 10% or more. When it comes to realistic values for the critical energy release rate, as in common cases of fiber-reinforced plastics, these may be expected to be of order one or higher. Thus, the cracks

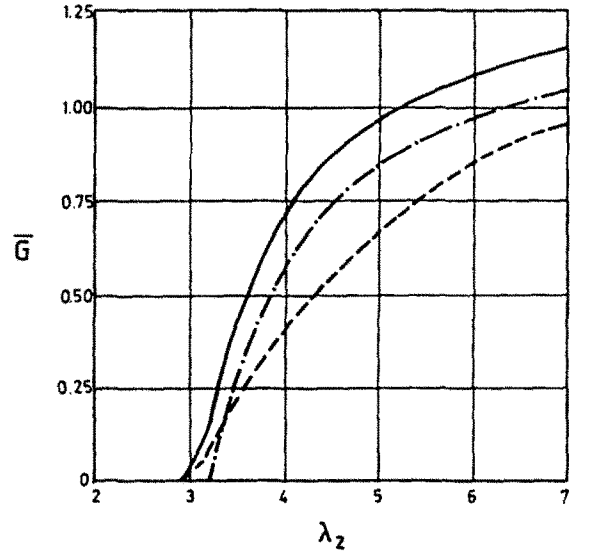

Fig. 5. Energy release rates, $\bar{G} = G/E_1 t_1 \varepsilon_0^2$, as a function of non-dimensional edge displacement, λ_2, for a plate with two delaminations, $E_1 = E_2$, $\nu_1 = \nu_2 = 0.3$, $a_1 = a_2$, $t_2 = 1.1t_1$; (– – –) lower crack 1, (——) upper crack 2 and (— · —) crack 2 with contact suppressed.

analyzed in connection with Fig. 5 will be expected to propagate in an unstable manner when λ_2 takes on values of around twice the buckling load. Transverse deflections as shown in Fig. 4 will then be critical at approximately three times the laminate thickness. Contact will be continuous at higher deflections although it will be lost at the centre of the plates for values of λ_2 being approximately 6 or larger.

It is then suitable to concentrate on the behavior of the energy release rate for different lengths of laminates and slightly different materials. In Fig. 6, again two delaminations are present although in this case the layers are equally thick and made of isotropic materials though with different Poisson ratios. The values for $\bar{G}$ for the two cracks are then depicted as functions of the crack length ratio for two different values of the outer loading.

If the applied load is just slightly above the buckling load, $\lambda_2 = 1.2\lambda_2^{cr}$, the values of the energy release rates are fairly low and it is not likely that any one of the cracks will start to grow. As is evident, contact will not be in question unless the crack length ratio does not exceed approximately 0.95. The influence of contact is then, however, quite obvious and in this particular case contact might affect $\bar{G}$-values by up to 20%.

If the outer loading is higher, $\lambda_2 = 3\lambda_2^{cr}$ as in Fig. 6, no new fundamental issues are involved although the values of the energy release rates are now more realistic when crack growth is a likely event. It should be noted, however, that at this higher value of the outer loading contact will not occur until a crack length ratio of above 0.98.

It is well known from the results by Yin (1985) that if a single delamination starts to grow in the present situation the behavior is expected to be catastrophic. This might, however, not be the case for multiple delaminations if contact is involved. If the lower crack in Fig. 6, corresponding to the dotted line for $\bar{G}$-values, grows when contact is present the increase in contact pressure between the layers will actually cause the energy release rate to decrease for this delamination and crack arrest might occur. If on the other hand the upper crack is critical and starts to grow when contact is present, the contact pressure will decrease and also in this situation, for the upper delamination, the energy release rate will actually decrease so that crack arrest might take place.

The analysis also shows that with a crack length ratio a_1/a_2 approaching unity, a discontinuity appears for $\bar{G}_1$. This phenomenon is believed to be anomalous and due to the use of plate variables. As a consequence a full 3D-analysis, or at least thick plate theory,

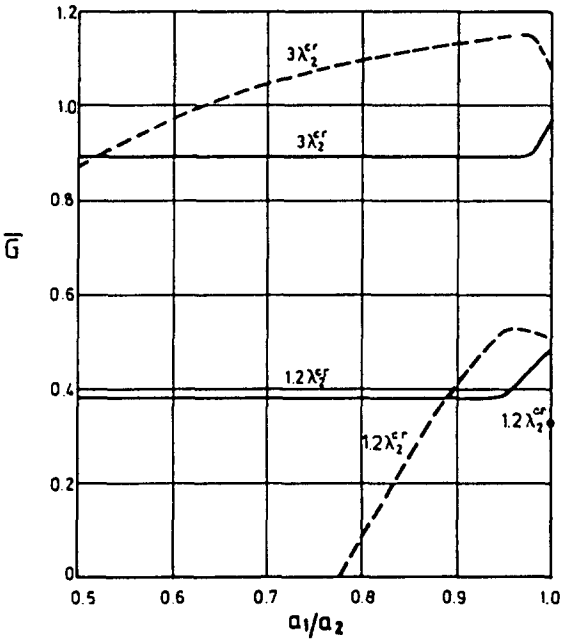

Fig. 6. Energy release rates, $\bar{G} = G/E_1 t_1 \varepsilon_0^2$, as a function of crack length ratio, a_1/a_2, for a plate with two delaminations, $E_1 = E_2$, $\nu_1 = 0.35$, $\nu_2 = 0.2$, $t_1 = t_2$, $\lambda_2 = 1.2\lambda_2^{cr}$ and $\lambda_2 = 3\lambda_2^{cr}$; (– – –) lower crack 1, (——) upper crack 2 and (●) $\bar{G}_1$ at $a_1 = a_2$.

seems necessary for a more accurate description of the multiple delamination problem in this situation. In the case of $\lambda_2 = 1.2\lambda_2^{cr}$, as shown in Fig. 6, the discontinuity gave a conservative result from a crack growth point of view while for $\lambda_2 = 3\lambda_2^{cr}$ the result proved to be substantially non-conservative, viz. $\bar{G}_1 = 1.75$. Thus, the whole feature must be considered as a drawback when relying on the use of plate variables at crack lengths being nearly equal.

Figure 7 illustrates energy release rates when a third delamination is introduced, depicted as a function of the crack length ratio a_1/a_2 though supplemented with an additional laminate with the crack length ratio a_2/a_3 fixed at 0.98. The three layers involved are assumed equally thick but have three different values of Poisson's ratio. The outer loading is taken as $\lambda_3 = 2\lambda_1^{cr}$.

With the results from Fig. 6 in mind, the behavior of the energy release rates shown in Fig. 7 is similar when contact between the layers enters the problem. For the two upper delaminations $\bar{G}$ increases while the lowest layer is forced down by the contact pressure and the energy release rate for this crack accordingly decreases. Again a conservative discontinuity for $\bar{G}_1$ is present at $a_1 = a_2$.

When the difference in thickness between layers is fairly large, as expected the effect of contact proves to be more pronounced than for the cases shown earlier in Figs 6 and 7. In Fig. 8, energy release rates are shown again as functions of the crack length ratio a_1/a_2. In this case, two delaminations are considered with a thickness of the upper layer being 1.5 times the lower one. The layers are assumed to have the same Poisson's ratio and Young's modulus for the upper layer being either equal to or twice the value of the lower one. The outer loading is fixed to $\lambda_2 = 2\lambda_2^{cr}$ and again the situation is as described in Figs 3b and 3d.

The effect of contact on energy release rates is perhaps surprisingly high as $\bar{G}_2$ is increased with more than 30% when contact is present. The difference in energy release rates for the lower layer at the two values of Young's modulus proved to be very small. In the present case, the discontinuity of $\bar{G}_1$ at cracks of equal length gave a significantly higher and non-conservative result for the energy release rate in contrast to some of the earlier findings for layers of equal thickness.

It is now appropriate to analyze in more detail the role of transverse displacements

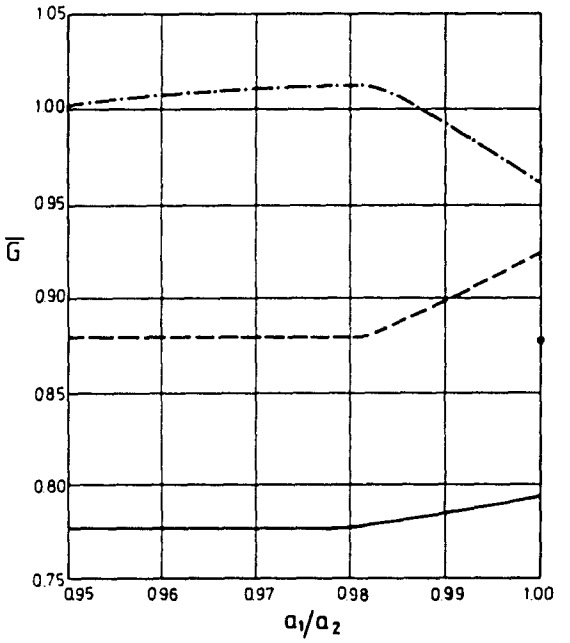

Fig. 7. Energy release rates, $\bar{G} = G\,E_1 t_1 \varepsilon_0^2$, as a function of crack length ratio, a_1/a_2, for a plate with three delaminations, $E_1 = E_2 = E_3$, $\nu_1 = 0.35$, $\nu_2 = 0.275$, $\nu_3 = 0.2$, $a_1 = 1.017a_2$, a_2, $t_1 = t_2 = t_3$, $\lambda_3 = 2\lambda_1^{cr}$; (— · —) lowest crack 1, (– – –) intermediate crack 2, (——) upper crack 3 and (●) G_1 at $a_1 = a_2$.

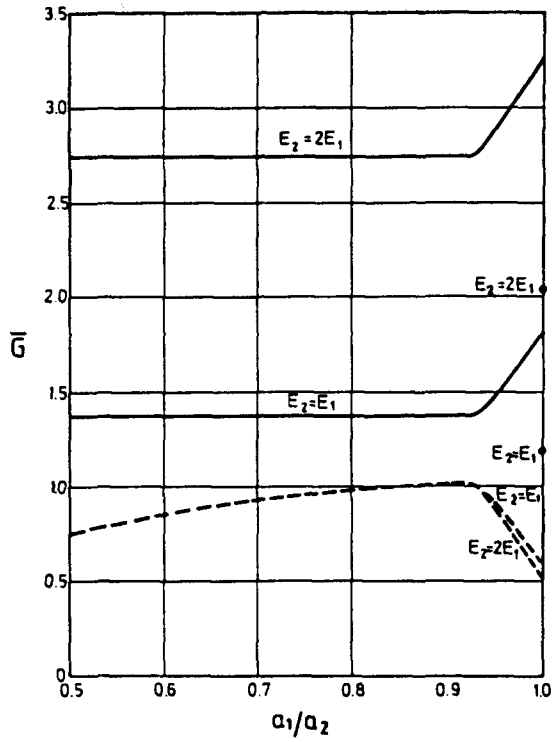

Fig. 8. Energy release rates, $\bar{G} = G/E_1 t_1 \varepsilon_0^2$, as a function of crack length ratio, a_1/a_2, for a plate with two delaminations, $E_2 = E_1$, and $E_2 = 2E_1$, $\nu_1 = \nu_2 = 0.3$, $t_2 = 1.5t_1$, $\lambda_2 = 2\lambda_2^{cr}$; (– – –) lower crack 1, (——) upper crack 2 and (●) $\bar{G}_1$ at $a_1 = a_2$.

and contact areas. Results are shown in Figs 9–11 for the case of two layers having the same material properties and the same geometry as in Fig. 8. The crack length ratio a_1/a_2 was fixed at unity while the outer loading was the parameter being varied. The problem posed was then analogous to that depicted in Figs 3c and 3d. It did prove possible, however, to find equilibrium solutions for non-zero transverse displacements only when the outer loading was larger than the buckling load for the upper layer. This is most likely due to

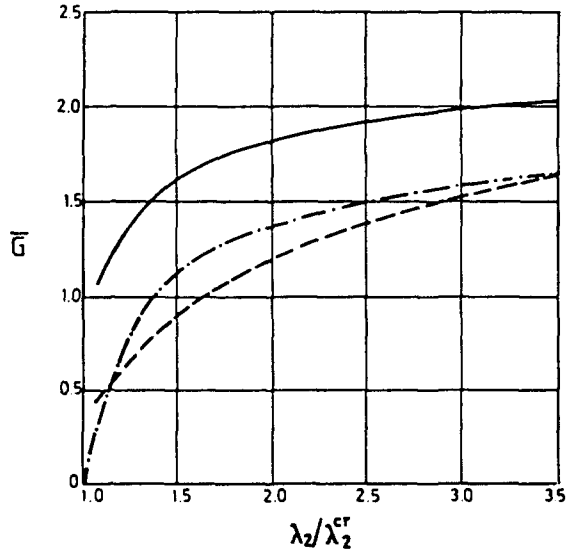

Fig. 9. Energy release rates, $\bar{G} = G/E_1 t_1 \varepsilon_0^2$, as a function of normalized edge displacement, λ_2/λ_2^{cr}, for a plate with two delaminations, $E_1 = E_2$, $\nu_1 = \nu_2 = 0.3$, $a_1 = a_2$, $t_2 = 1.5t_1$; (– – –) lower crack 1, (——) upper crack 2 and (— · —) crack 2 with contact suppressed.

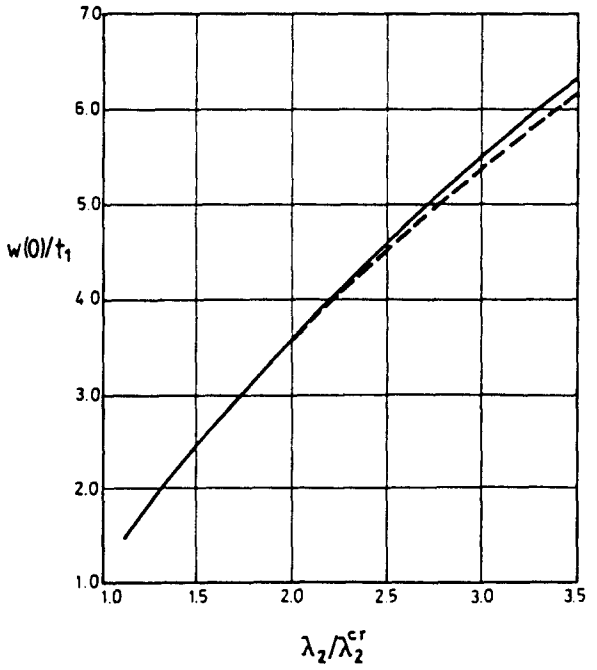

Fig. 10. Transverse displacements, $w(0)/t_1$, as a function of normalized edge displacement, λ_2/λ_2^{cr}, for a plate with two delaminations, $E_1 = E_2$, $\nu_1 = \nu_2 = 0.3$, $a_1 = a_2$, $t_2 = 1.5t_1$; (- - -) lower crack 1 and (——) upper crack 2.

numerical inadequacies caused by a very high stiffness of the upper layer until the outer loading reaches the buckling load for this member.

In Fig. 9, energy release rates are depicted as functions of the normalized outer loading parameter λ_2/λ_2^{cr}. The conclusions drawn are similar to those related to Fig. 5 with a smaller

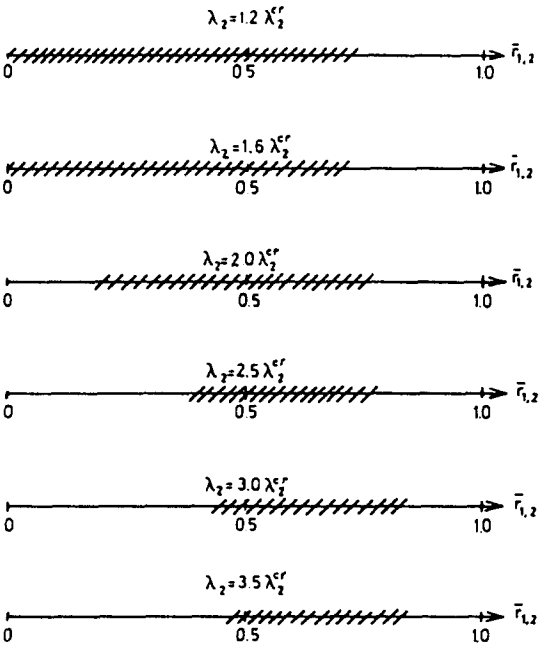

Fig. 11. Contact area (shaded) for layers in a plate with two delaminations for different values of normalized edge displacement λ_2/λ_2^{cr}, $E_1 = E_2$, $\nu_1 = \nu_2 = 0.3$, $a_1 = a_2$, $t_2 = 1.5t_1$.

thickness ratio and it is evident in this case that to a substantial degree, energy release rates are underestimated when contact is not taken into account.

In Fig. 10, transverse displacements in the center of the layers are plotted as a function of the outer loading. As may be seen, local contact is present at $\bar{r} = 0$ up to about twice the buckling value and subsequently the contact region becomes annular. Such contact behavior did occur also for the upper layer being somewhat thinner, as in Fig. 4. The difference in transverse displacements at the center was, however, fairly small for the two layers even at high values of the outer load.

The development of the contact area is depicted in Fig. 11 for increasing values of the outer loading. As has been indicated earlier, it is interesting to note that the contact area is moving away from the center of the layers and also becomes smaller as the outer loading is increased.

In order to also investigate the effect of a large number of cracks, some illustrative solutions are shown in Fig. 12. In this case equally long delaminations, at most five, with a small difference in thickness are considered, this is to ensure that contact will occur between all layers present. All plates are made of the same material though with increasing thickness and the outer loading corresponding to twice the buckling load for the uppermost layer, i.e. $\lambda_5 = 2\lambda_5^{cr}$.

Chai *et al.* (1981) and Chai and Babcock (1985) have conjectured that mostly it is sufficient in similar multiple delamination problems to take into account only a single delamination. With contact considered, the results depicted in Fig. 12 show, however, that with a small number of cracks (presently four or less) the most critical delamination from a crack growth point of view is the uppermost one while for an additional delamination the lowest crack becomes the most critical one. Remembering that energy release rates are very material and geometry dependent, the results shown in Fig. 12 indicate the need to analyze the behavior of all cracks present in the damaged structure with contact included in order to clarify the crack growth behavior in multiple delamination problems.

Finally the influence of the tolerance of contact on the convergence of the solution has been analyzed. The parameter ε, as defined in (11), corresponds to the relative magnitude of the interpenetration between two layers in contact. Figure 13 shows the results for the case of a plate with two delaminations of equal length and material, but with the upper layer 50% thicker than the lower one. The outer loading was taken to be twice the buckling load for the upper layer. For this particular geometry convergence was reached at ε being approximately equal to 5×10^{-3} and in other studies, indicating that tolerances around 10^{-3} were acceptable in almost every case dealt with.

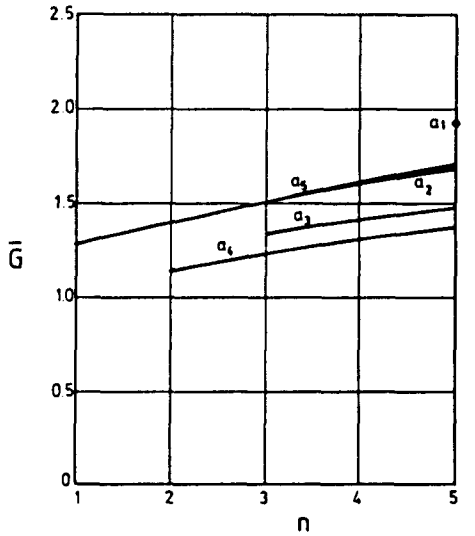

Fig. 12. Energy release rates, $\bar{G} = G/E_1 t_1 \varepsilon_0^2$, as a function of number of delaminations, n, in a plate. $E_1 = E_2 = E_3 = E_4 = E_5$, $\nu_1 = \nu_2 = \nu_3 = \nu_4 = \nu_5 = 0.3$, $a_1 = a_2 = a_3 = a_4 = a_5$, $t_2 = 1.1t_1$, $t_3 = 1.2t_1$, $t_4 = 1.3t_1$, $t_5 = 1.4t_1$, $\lambda_5 = 2\lambda_5^{cr}$.

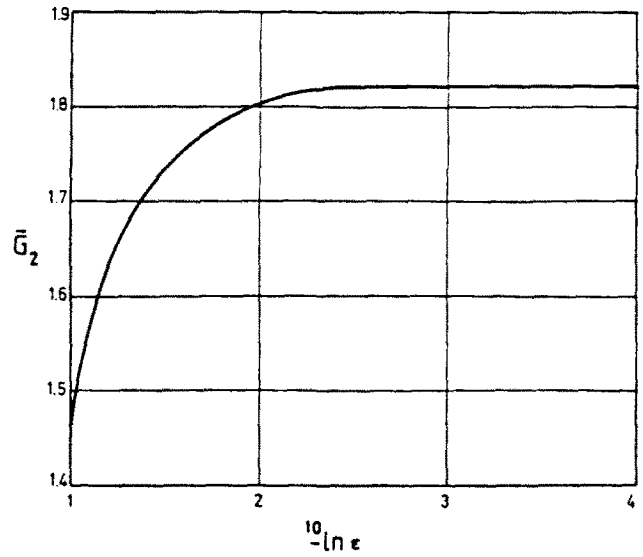

Fig. 13. Energy release rate, $\bar{G}_2 = G_2/E_1 t_1 \varepsilon_0^2$, as a function of the tolerance, ε defined in (11), for a plate with two delaminations, $E_1 = E_2$, $\nu_1 = \nu_2 = 0.3$, $a_1 = a_2$, $t_2 = 1.5t_1$, $\lambda_2 = 2\lambda_2^0$.

6. CONCLUSIONS

An effort was made to investigate the interaction between buckled delaminated layers and the resulting features as regards possible crack growth. As the outcome naturally rests on several simplifying assumptions, though still found complex, a balance was sought for to bring out the salient features due to crack growth in the presence of multiple delaminations subjected to contact. Under these conditions, results were generally found to be non-conservative when compared to single delaminations experiencing no contact between layers, but still being subject to catastrophic crack growth.

In the first situation explicitly dealt with, involving two interacting delaminations with the thicker layer being forced to deflect by a buckled thinner one, a higher energy release rate will result for the thicker member. As a consequence, crack growth might be possible in situations where a single member is still below the buckling load. Also, at nominal buckling of both layers the energy release rate will be increased for the upper crack, as compared to a single delamination when contact is caused by a thinner member. When laminates are of closely similar stiffness and differ in length by only a few per cent, the energy release rate may be changed by up to 20% due to contact. When one member is 50% thicker, the influence of contact on the energy release rate is of order one and the effect is definitely of importance. The situation was similar for three interacting laminates.

Although cases of primarily two delaminations have been dealt with, it was evident that no simple conclusions may be drawn about growth behavior without a detailed analysis. This finding was true also in the case of an increasing number of laminates, up to five, and having contact between all layers. No continuous behavior of delamination growth was predicted but instead all cases had to be analyzed in detail.

All results were based on plate theory which caused an anomalous discontinuity in the energy release rate at approaching crack lengths. It would seem of interest to study this issue further by using the three-dimensional theory.

Acknowledgements—I would like to thank Professor Bertil Storåkers for his willingness to give helpful advice.

REFERENCES

Bolotin, V. V., Zebelyan, Z. K. and Kurzin, A. A. (1981). Stability of compressed components with delamination-type flaws. *Probl. Proch.* **7**, 813–819.

Chai, H. and Babcock, C. D. (1985). Two-dimensional modelling of compressive failure in delaminated laminates. *J. Compos. Mater.* **19**, 67–98.

Chai, H., Babcock, C. D. and Knauss, W. G. (1981). One dimensional modelling of failure in laminated plates by delamination buckling. *Int. J. Solids Structures* **17**, 1069–1083.
Larsson, P.-L. (1990). On delamination buckling and growth in circular and annular orthotropic plates. *Int. J. Solids Structures* **27**(1), 15–28.
Storåkers, B. (1989). Nonlinear aspects of delamination in structural members. *Proc.* XVIIth *Int. Congress Theoretical Applied Mechanics*, pp. 315–336. Elsevier, Amsterdam.
Storakers, B. and Andersson, B. (1988). Nonlinear plate theory applied to delamination in composites. *J. Mech. Phys. Solids* **36**, 689–718.
Strang, G. (1986). *Introduction to Applied Mathematics*. Wellesley–Cambridge, Wellesley.
Suo, Z. and Hutchinson, J. W. (1988). Interface crack between two elastic layers. *Int. J. Fracture* **43**, 1–18.
Wang, S. S., Zahlan, N. M. and Suemasu, H. (1985a). Compressive stability of delaminated random short-fiber composites, Part I—Modeling and methods of analysis. *J. Compos. Mater.* **19**, 296–316.
Wang, S. S., Zahlan, N. M. and Suemasu, H. (1985b). Compressive stability of delaminated random short-fiber composites, Part II—Experimental and analytical results. *J. Compos. Mater.* **19**, 317–333.
Yin, W.-L. (1985). Axisymmetric buckling and growth of a circular delamination in a compressed laminate. *Int. J. Solids Structures* **21**, 503–514.

APPENDIX

The elements appearing in the matrix equation (14) are explicitly

$$K_{11} = \int_0^1 [\{N'\}^T\{N'\} + \nu[\{N'\}^T\{N\} + \{N\}^T\{N'\}]/\bar{r} + \{N\}^T\{N\}/\bar{r}^2]\bar{r}\,\mathrm{d}\bar{r},$$

$$K_{12} = \int_0^1 (\bar{w}'\{\bar{r}N' + \nu N\}^T\{N'\})\,\mathrm{d}\bar{r},$$

$$K_{22} = \int_0^1 \{[\{N''\}^T\{N'\} + \nu[\{N''\}^T\{N'\} + \{N'\}^T\{N''\}]/\bar{r} + \{N'\}^T\{N'\}/\bar{r}^2]/12 + (\bar{u}' + 3\bar{w}'^2/2 + \nu\bar{u}/\bar{r}) \cdot \{N'\}^T\{N'\}\}\bar{r}\,d\bar{r},$$

$$R_1 = -\int_0^1 [\bar{u}'\{N'\}^T + \nu[\bar{u}'\{N\}^T + \bar{u}\{N'\}^T]/\bar{r} + \bar{u}\{N\}^T/\bar{r}^2 + \bar{w}'^2(\{N'\}^T + \nu\{N\}^T/\bar{r})/2]\bar{r}\,\mathrm{d}r,$$

$$R_2 = \int_0^1 \{(1-\nu^2)\bar{q}\{N'\}^T - [\bar{w}''\{N''\}^T + \nu[\bar{w}'\{N''\}^T + \bar{w}''\{N'\}^T]/\bar{r} + \bar{w}'\{N'\}^T\bar{r}^2]/12$$
$$+ \bar{w}'(\bar{u}' + \bar{w}'^2/2 + \nu\bar{u}/\bar{r})\{N'\}^T\}\bar{r}\,\mathrm{d}\bar{r}.$$